Pergamon

Int. J. Solids Structures Vol. 35, Nos. 1–2, pp. 33–49, 1998

0020–7683/98 $19.00 + .00

PII: S0020–7683(97)00046–2

EFFECTS OF STRAIN FIELD ON LIGHT IN CRACK OPENING INTERFEROMETRY

JEFFREY W. KYSAR
Division of Engineering and Applied Sciences, Harvard University, Pierce Hall, Cambridge, Massachusetts 02138, U.S.A.

(*Received* 4 *September* 1996, *in revised form* 21 *January* 1997)

Abstract—Crack opening interferometry is a standard technique used to measure the normal opening displacement profile of a crack in a transparent material. This paper calculates how much an incident light ray deflects from a nominally straight line path due to strain induced changes in the index of refraction.

It is shown that an incident plane wavefront of light that propagates toward a plane strain crack is split into two linearly polarized light rays: one polarized in a direction parallel to the crack front; the other polarized in the plane perpendicular to the crack front.

Assuming linear, elastic mechanical behavior and linear optical behavior in a homogeneous, isotropic medium, the index of refraction of both wavefronts is derived for a Mode I crack in the K-field region. In general, the index of refraction is anisotropic and inhomogeneous. Four new material parameters are identified which characterize crack opening interferometry; values are tabulated for three materials.

Using geometrical optics, the paths of both light rays are calculated analytically for a special set of initial conditions and an expression for the total light deflection at the crack flank is obtained.

The results show that for some materials and specimen geometries, the absolute deflection of each light ray is large enough to be measured, but the relative deflection (i.e. the difference in deflection between the two light rays) is too small to be measured. The main effect that this phenomenon has on crack opening interferometry is to cause a shift in the apparent position of the crack tip. It is shown that this shift will not affect the interpretation of the interference fringes in terms of crack opening displacement. © 1997 Elsevier Science Ltd.

1. INTRODUCTION

Crack opening interferometry is a standard technique (Liechti, 1993) used to measure the normal opening displacement profile of a crack in a transparent material or of a crack along the interface of a bimaterial system that has at least one transparent component. The technique, as illustrated in Fig. 1, consists of shining a light through the transparent material to the crack flanks. Light reflecting from both flanks interferes to form a set of interference fringes. The difference in optical path length of the two wavefronts of light depends on the distance between the crack flanks. Therefore, the results can be interpreted in terms of normal crack opening displacement. In the present study, the incoming light wavefront is assumed to be normal to the crack flanks in the unstrained configuration.

The index of refraction is a function of the strain state, however, so complications arise when light passes through the region of stress and strain concentration around the crack tip. This causes the incident light to deviate from a straight line path.

Fowlkes (1975) analyzed the path of incident light in the vicinity of a crack tip in cast acrylic assuming the Mode I singular elastic field and concluded that the light ray does significantly deflect from a straight line path. (A significant deflection, here, is defined as one large enough to be measured by an optical instrument with a spatial resolution of approximately 1×10^{-6} m.) A similar analysis (Liang and Liechti, 1995) predicted that, under the same Mode I loading and stress intensity factor, the light path in the vicinity of a crack in BK-7 glass does not deflect significantly. Both studies used the same approximate, empirical relationship between applied load and index of refraction. The analyses differed only in the material properties used in the numerical simulations.

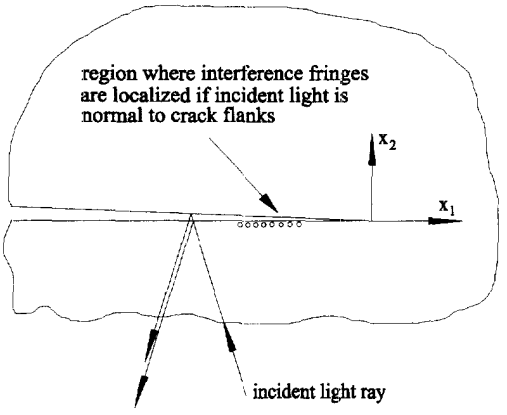

Fig. 1. Schematic of crack opening interferometry.

The goal of this paper is to analyze the behavior of incident light as it traverses a transparent medium leading up to the crack flanks and to calculate, both analytically and numerically, the path of the light near a crack tip under Mode I loading. It is assumed that the medium is mechanically isotropic and homogeneous and is optically isotropic and homogeneous in its unstrained state.

Section 2 reviews the well-established behavior of light in both naturally and mechanically birefringent solids. A general conclusion is that two wavefronts of light can propagate independently along any given direction of an optically anisotropic medium. Further, for each individual wave front, the direction of wavefront propagation and the direction of energy flow (i.e. the light ray direction) associated with the wavefront do not, in general, coincide. Also, a material that is optically isotropic can become anisotropic if it is mechanically deformed.

In Section 3, the general features of light propagation in the near tip region of a plane strain crack are identified. It is shown that if one assumes plane strain conditions, a wave front of light is, in general, split into two linearly polarized wavefronts: one polarized parallel to the crack front; the other polarized in a plane perpendicular to the crack front. In addition, it is shown that the index of refraction of the wavefront polarized parallel to the crack front is a function, only, of position. However, the index of refraction of the wavefront polarized in a plane perpendicular to the crack front is a function of both position and direction of propagation. Hence, in general, the calculation of the light path reduces to that of electromagnetic wave propagation in an anisotropic, inhomogeneous medium.

In Section 4, the index of refraction as a function of applied load is derived for each wavefront assuming linear optical theory and the singular Mode I strain field of linear, isotropic elasticity. Four new material parameters are identified which characterize crack opening interferometry; values of the parameters are tabulated for three commonly used materials.

Section 5 reviews the general equations of geometrical optics which govern the propagation of electromagnetic waves in an anisotropic, inhomogeneous medium in the limit of vanishing wavelength and shows that the direction and speed of wavefront propagation is governed by the index of refraction. This complicates the problem conceptually because the goal of this paper is to calculate the path of the light ray, but the index of refraction determines the direction of wavefront propagation and not of the light ray. However, the governing equations can be written in terms of a characteristic set of ordinary differential equations that provides the link between the direction of ray propagation and the direction of wavefront propagation.

In Section 6, the problem is formulated and solved analytically for the special case of a light wavefront that would, in an unloaded state, approach the crack in the direction perpendicular to the crack flanks and strike the crack tip. An analytic expression which

gives the total light deflection of both light rays at the crack tip is obtained in terms of the newly identified material parameters. In addition, the problem is solved numerically to investigate the behavior of light rays with other initial conditions.

Section 7 discusses the implications of these results on crack opening interferometry. First, it is important to note that the two light rays deflect different amounts. If the difference in deflection of the two light rays is large enough to be measured, in principle, one could directly obtain the value of the Mode I stress intensity factor without the need to measure the normal crack opening displacement. A drawback, though, is that an observer would record a double image of the fringes which could lead to erroneous normal crack opening displacement results. It is shown that for the materials and geometries considered in this paper, the effect is too small to be measured.

Section 8 summarizes the results.

2. BEHAVIOR OF LIGHT IN AN OPTICALLY ANISOTROPIC MEDIUM

The theory of light propagating in an anisotropic, homogeneous medium is well developed. This section will review the concepts necessary to understand the developments of this paper. The interested reader can fine a complete derivation starting from Maxwell's equations in Born and Wolf (1993).

If one assumes that light is propagating through a non-magnetic, transparent (implies negligible specific conductivity), medium that has no electric charge density, the only non-zero quantities that enter into Maxwell's equations are: **D**, the electric displacement vector; **B**, the magnetic induction vector; **E**, the electric vector; and **H**, the magnetic vector. If the medium is linear, the constitutive relations between these quantities are

$$\mathbf{B} = \mu_0 \mathbf{H}$$

$$\mathbf{D} = \varepsilon_0 \overrightarrow{\overrightarrow{\varepsilon}} \cdot \mathbf{E} \tag{1}$$

where

$$\langle \mu_0 = \text{magnetic permeability of free space} \rangle$$

$$\langle \varepsilon_0 = \text{dielectric permittivity of free space} \rangle$$

$$\langle \overrightarrow{\overrightarrow{\varepsilon}} = \text{relative dielectric permittivity} \rangle.$$

The magnetic permeability is isotropic and that of free space because the material is non-magnetic. The anisotropy enters the equations through the relative dielectric permittivity.

It is convenient to define the *slowness vector*, **p**, of the wavefront as $\mathbf{p} = n\mathbf{m}$, where: $n = c/v$ is the index of refraction of wavefront; $c^2 = 1/\varepsilon_0\mu_0$ is speed of light in free space; v is the speed of wavefront of light in the anisotropic medium; and **m** is the unit vector in the direction of propagation.

For an arbitrary direction of propagation, Maxwell's equations predict two separate wave speeds. This implies that two independent, linearly polarized wavefronts can propagate in any given direction. Such a "double refracting" medium is said to be *birefringent*. The principal values of $\overrightarrow{\overrightarrow{\varepsilon}}$ determine the two possible wave speeds. As an example, if we choose position coordinates that coincide with the principle axes of $\overrightarrow{\overrightarrow{\varepsilon}}$ and a wavefront that propagates in the $\mathbf{m} = (0, 0, 1)$ direction, the magnitudes of the two possible slowness vectors (i.e. the two possible indices of refraction) are $(p)_1 = n_1 = \sqrt{\varepsilon_{11}}$ and $(p)_2 = n_2 = \sqrt{\varepsilon_{22}}$.

Maxwell's equations show that **D** is transverse to the direction, **m**, of wavefront propagation and that the principal axes of $\overrightarrow{\overrightarrow{\varepsilon}}$ determine the planes of polarization (i.e. the directions of **D**). In this example, the wavefront with index of refraction n_1 is polarized in the x_1–x_3 plane. The wavefront with index of refraction n_2 is polarized in the x_2–x_3 plane.

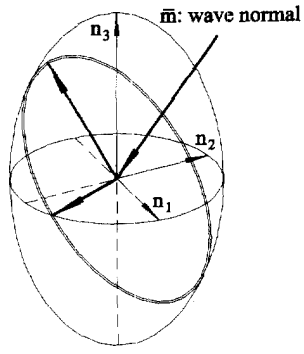

Fig. 2. Index ellipsoid.

If the direction of propagation is oblique to a principal direction of $\overleftrightarrow{\varepsilon}$, a geometrical construction called the *index ellipsoid* can be used to calculate the two indices of refraction and planes of polarization. Using the same principal axis position coordinates, we define the *principal refractive indices*, n_α, as

$$n_\alpha = \sqrt{\varepsilon_{\alpha\alpha}} = \sqrt{\frac{1}{B_{\alpha\alpha}}}, \quad (\alpha = 1,2,3), \text{no summation} \tag{2}$$

where

$$\overleftrightarrow{B} = \overleftrightarrow{\varepsilon}^{-1} = \text{relative dielectric impermeability.}$$

Note that, by convention, $\overleftrightarrow{B}$ and **B** are denoted by the same letter; the meaning should be clear from context. The index ellipsoid is then defined as

$$\frac{x_1^2}{n_1^2} + \frac{x_2^2}{n_2^2} + \frac{x_3^2}{n_3^2} = 1. \tag{3}$$

As demonstrated schematically in Fig. 2, one can find the indices of refraction and the planes of polarization associated with a given direction of propagation by forming the elliptical cross-section of the index ellipsoid that is parallel to the light wavefront and passes through the center of the index ellipsoid. The lengths of the semi-axes of the elliptical cross-section are equal to the indices of refraction, and the directions indicate those of polarization.

The shape of the index ellipsoid must contain the same symmetry elements as the crystalline structure of the medium (Nye, 1972). As a result, the optical properties are classified as being anaxial, uniaxial, or biaxial depending upon whether, respectively, all, two, or none of the principal refractive indices are equivalent. In an optically anaxial medium, the index ellipsoid reduces to a sphere; such a medium is said to be optically isotropic.

Another general feature of wave propagation in anisotropic media is that the *light ray* (i.e. the electromagnetic energy associated with a wavefront) does not, in general, propagate in the same direction as the wavefront. The electromagnetic energy flows in the direction of the Poynting vector defined as $\mathbf{S} = \mathbf{E} \times \mathbf{H}$. From Maxwell's equations we can see that **H** is perpendicular to **m** and to **D**, whereas **E** lies in the plane of **m** and **D**, so that **S** is also in the plane of **m** and **D**. In isotropic media, the direction of wavefront propagation coincides with the direction of the light ray. In anisotropic media, one must be careful to distinguish between the path of a wavefront of light and the path of a light ray.

An optically isotropic material can become anisotropic if it is strained. The relationship between the relative dielectric impermeability tensor and strain tensor is expressed in

terms of the 4th order *elasto-optic tensor*, p_{ijkl}. The conventional way of quantifying this relationship (Nye, 1972) is, for an optically and mechanically isotropic material

$$\begin{bmatrix} \Delta B_1 \\ \Delta B_2 \\ \Delta B_3 \\ \Delta B_4 \\ \Delta B_5 \\ \Delta B_6 \end{bmatrix} = \begin{bmatrix} p_{11} & p_{12} & p_{12} & 0 & 0 & 0 \\ p_{12} & p_{11} & p_{12} & 0 & 0 & 0 \\ p_{12} & p_{12} & p_{11} & 0 & 0 & 0 \\ 0 & 0 & 0 & p & 0 & 0 \\ 0 & 0 & 0 & 0 & p & 0 \\ 0 & 0 & 0 & 0 & 0 & p \end{bmatrix} \begin{bmatrix} \varepsilon_1 \\ \varepsilon_2 \\ \varepsilon_3 \\ \varepsilon_4 \\ \varepsilon_5 \\ \varepsilon_6 \end{bmatrix} \tag{4}$$

where

ΔB_m = change in relative dielectric impermeability tensor

$\langle p_{11}, p_{12}$ = elasto-optical coefficients$\rangle$

$\left\langle p = \frac{1}{2}(p_{11} - p_{12}) \right\rangle$

$\langle \varepsilon_n$ = elastic strain$\rangle$.

Again, there is a potential for confusion from the notation. It is conventional to denote both the relative dielectric impermeability tensor and strain tensor as $\vec{\vec{\varepsilon}}$; the meaning should be clear from the context. The elasto-optic coefficients are of order $O(10^{-1})$ and are dimensionless. Nye (1972) discusses how the tensor and matrix forms are interchanged.

After finding the principal values and directions of $\vec{\vec{B}}$, the approximate change in principal indices of refraction can be found by differentiating (2) to yield $\Delta n_\alpha \approx -(n_\alpha^0)^3 \Delta B_\alpha/2$ ($\alpha = 1, 2, 3$ corresponding to principal values), where Δn_α is the change in principal index of refraction and n_α^0 is the unstrained principal index of refraction. The principal indices of refraction are then $n_\alpha = n_\alpha^0 + \Delta n_\alpha$.

At this point we should note one assumption that has been made implicitly. Strictly speaking, the index of refraction is a function of the displacement gradient tensor, rather than the strain tensor (Günter and Zgonik, 1991). This becomes evident if one realizes that the orientation of the index ellipsoid is determined by the underlying crystal structure. Since the rotation field associated with the anti-symmetric part of the displacement gradient causes the crystal structure to rotate, the index ellipsoid also rotates relative to its undeformed state. The effects of the strain field on the index ellipsoid must be calculated in this "rotated" state.

However, if the medium is optically and mechanically isotropic in the undeformed state, both the unstrained $\vec{\vec{B}}$ tensor and the p_{ijkl} tensor are invariant to rotation and (4) suffices to calculate the change of index of refraction.

3. LIGHT PROPAGATION IN NEAR CRACK TIP REGION

The index ellipsoid determines both the plane of polarization as well as the index of refraction of each wavefront of light. Therefore, one can determine the general properties of light propagating in the near crack tip region by finding the orientation of the relative dielectric impermeability tensor (and hence, the index ellipsoid) relative to the crack.

To that end, we assume that a semi-infinite plane strain crack exists in a mechanically and optically isotropic medium and that the system is loaded by some combination of Mode I and Mode II. Figure 3 shows the cross-section of the index ellipsoid in the x_1–x_2 plane. The crack front coincides with the x_3-axis. The angle ω specifies the direction of the wavefront normal of light propagating in the x_1–x_2 plane. The position of the wavefront normal is specified by r and θ.

The only non-zero strains are ε_{11}, ε_{12}, $\varepsilon_{22} \neq 0$, so from (4), $\vec{\vec{B}}$ will change only in ΔB_1, ΔB_2, ΔB_3, and ΔB_6. Since an off-diagonal term exists, the principal axes of the index ellipsoid

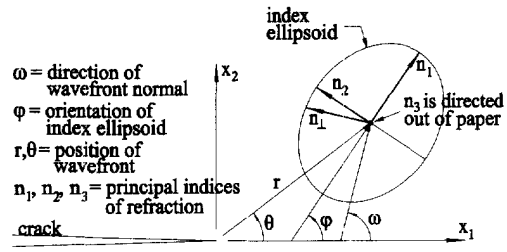

Fig. 3. Index ellipsoid relative to plane strain crack.

are not parallel to the coordinate axes. The ΔB_6 term causes the principal axes of the index ellipsoid to be rotated in the x_1–x_2 plane, with one principal axis of the index ellipsoid parallel to the x_3-axis. As shown in Fig. 3, we assign the principal indices of refraction n_1 and n_2 to be in the x_1–x_2 plane and the other, n_3, to be parallel to the x_3-axis. The angle φ represents the orientation of n_1 in the x_1–x_2 plane and is determined by the ΔB_6 term; when $\varphi = 0$, n_1 is parallel to the x_1-axis.

The principal indices of refraction and the orientation of the index ellipsoid are functions are position because they depend only upon the optical properties and the inhomogeneous strain state.

Although up to this point we have made no detailed calculations, it is possible to find the polarizations of an incident wavefront of light travelling in a direction, ω, in the x_1–x_2 plane. If the index ellipsoid construction of Section 2 is applied to Fig. 3, it is evident that one wavefront will be polarized in a plane parallel to the crack front and experience an index of refraction which will be denoted $n_\parallel$. The other semi-axis of the elliptical cross-section lies in the x_1–x_2 plane. This wavefront will be polarized in a plane perpendicular to the crack front and experience an index of refraction which will be denoted $n_\perp$. Henceforth, the two wavefronts will be called the *parallel wavefront* and the *perpendicular wavefront*, respectively. Both wavefronts are confined to the x_1–x_2 plane because of the plane strain conditions.

It is also possible to find the functional form of $n_\parallel$ and $n_\perp$ from the geometry of the index ellipsoid in Fig. 3. The semi-axis denoted by $n_\perp$ changes length if the direction of light propagation changes (i.e. if ω changes). Therefore $n_\perp$ is a function of both position, $\mathbf{x}$, as well as the direction of propagation, $\mathbf{m}$. The index of refraction $n_\parallel$ is equal to n_3 and, therefore, is a function only of position, and not of $\mathbf{m}$.

The functional forms of the indices of refraction are

$$n_\perp = n_\perp(\mathbf{x}, \mathbf{m})$$
$$n_\parallel = n_\parallel(\mathbf{x}). \tag{5}$$

Since $n_\perp$ is a function of both position and direction, the problem of calculating the path of light in the near crack tip region reduces to that of electromagnetic wave propagation in an anisotropic, inhomogeneous medium.

4. INDICES OF REFRACTION

As stated in the previous section, the index of refraction of the parallel wavefront is $n_\parallel = n_3$. From Fig. 3 it can be shown that the radius of the ellipse denoted by $n_\perp$ is

$$n_\perp^2 = \frac{1}{2}(n_1^2 + n_2^2) - \frac{1}{2}(n_1^2 - n_2^2)\cos[2(\omega - \varphi)]. \tag{6}$$

Now that we have the precise functional forms for $n_\perp$ and $n_\parallel$, the next step is to obtain n_1, n_2, n_3 and φ. We assume that a plane strain crack exists in a medium in which the mechanical and optical properties are isotropic and homogeneous in its undeformed state,

so that we need consider only the effect of the strain state. Further, we consider only the contribution from the singular Mode I elastic strain field.

From the known strain field (e.g. Kanninen and Popelar, 1985) and (4), we calculate the change in relative dielectric impermeability and add to the unstrained isotropic value B to obtain $\overleftrightarrow{B}$ in matrix from

$$\overleftrightarrow{B} = \begin{pmatrix} B' - \Delta B_6 \tan(3\theta/2) & \Delta B_6 & 0 \\ \Delta B_6 & B' + \Delta B_6 \tan(3\theta/2) & 0 \\ 0 & 0 & B'' \end{pmatrix} \tag{7}$$

where

$$\Delta B_6 = \frac{1}{\sqrt{2}}(p_{11} - p_{12}) q_1 r^{-1/2} \frac{\cos(\theta/2)\sin(\theta/2)\cos(3\theta/2)}{1-2\nu}$$

$$\left\langle B' = B + \frac{1}{\sqrt{2}}(p_{11} + p_{12}) q_1 r^{-1/2} \cos(\theta/2) \right\rangle$$

$$\langle B'' = B + \sqrt{2} p_{12} q_1 r^{-1/2} \cos(\theta/2) \rangle$$

and

$$\left\langle q_1 = \frac{(1-2\nu)(1+\nu)K_1}{E\sqrt{\pi}}, \quad (\text{SI units}: m^{1/2}) \right\rangle$$

$$\langle K_1 = \text{Mode I stress intensity factor} \rangle$$

$$\langle E = \text{Young's modulus} \rangle$$

$$\langle \nu = \text{Poisson's ratio} \rangle.$$

The principal values and principal axes of the index ellipsoid are determined from the eigenvalues and eigenvectors of $\overleftrightarrow{B}$. The eigenvalues, λ_i, are

$$\lambda_{1,2} = B\{1 + 2\sqrt{2} c_\perp q_1 r^{-1/2} [\cos(\theta/2) \pm \beta \sin(\theta)]\}$$

$$\langle \lambda_3 = B[1 + 2\sqrt{2} c_\parallel q_1 r^{-1/2} \cos(\theta/2)] \rangle \tag{8}$$

where

$$\left\langle c_\parallel = \frac{1}{2} p_{12} n_0^2 \right\rangle$$

$$\left\langle c_\perp = \frac{1}{4}(p_{11} + p_{12}) n_0^2 \right\rangle$$

$$\left\langle \beta = \frac{(p_{11} - p_{12})}{2(1-2\nu)(p_{11} + p_{12})} \right\rangle$$

and

$$n_0^2 = \frac{1}{B}.$$

The eigenvector associated with λ_3 is parallel to the x_3-axis so it corresponds to the parallel wavefront. The eigenvectors associated with λ_1 and λ_2 then must lie in the x_1–x_2 plane and contribute to the index of refraction of the perpendicular wavefront.

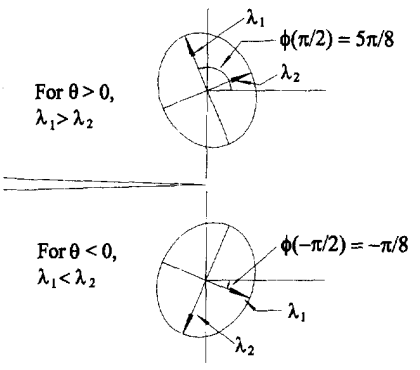

Fig. 4. Index ellipsoid at angles $\theta = \pm\pi/2$.

To fully characterize the index ellipsoid, it suffices to find the direction in the x_1–x_2 plane of the eigenvector associated with λ_1. It can be shown that this angle (as a function of position) is

$$\varphi = \frac{3\theta}{4} + \frac{\pi}{4}. \tag{9}$$

The results of the eigenproblem are summarized in Fig. 4 for $\theta = \pm\pi/2$. From (9) it is evident that the angle φ is not an even function. Also from (8), it is evident that for $\theta > 0$, $\lambda_1 > \lambda_2$ and that for $\theta < 0$, $\lambda_1 < \lambda_2$. Nevertheless, the quadric surface of $\vec{\vec{B}}$ maintains the mirror symmetry about the x_1-axis required by the pure Mode I loading.

Four material constants have been introduced. The first, q_I, depends on mechanical properties and the Mode I stress intensity factor. Two others $c_\parallel$ and $c_\perp$, depend exclusively on optical properties. The parameter, β, depends mainly on optical parameters but has a weak dependence on Poisson's ratio. As will become clear later, β is a measure of the *strain induced optical anisotropy*. If one assumes that in q_I the loading parameter K_I is replaced by the material property K_{IC} (i.e. the critical stress intensity factor in Mode I), q_I becomes the material property, q_{IC}. The properties (Watson, *et al.* 1994; Kalthoff, 1993; Lawn, 1993) are summarized in Table 1 for three materials commonly used in crack opening interferometry.

It is important to note that from (8) the change in length of the principal axes of $\vec{\vec{B}}$ is small for all $r \gg (c_\perp q_{IC})^2$. For the materials in Table 1, the change becomes large only when r is smaller than an atomic spacing. The important length scale is the wavelength of visible light which in free space is in the range of 0.4×10^{-6} to 0.7×10^{-6} meter.

Therefore, we can use (2) and (8) along with the binomial theorem to calculate the expressions for the principal indices of refraction.

$$\begin{aligned} n_{1,2} &= n_0\{1 - \sqrt{2}c_\perp q_I r^{-1/2}[\cos(\theta/2) \pm \beta \sin(\theta)]\} \\ n_3 &= n_\parallel = n_0[1 - \sqrt{2}c_\parallel q_I r^{-1/2}\cos(\theta/2)]. \end{aligned} \tag{10}$$

Finally, using (6) and (10), neglecting terms of order $O(c_\perp^2 q_I^2 r^{-1})$ and once again invoking the binomial theorem yields

Table 1. Optical properties for commonly used materials

Material	E (GPa)	ν	n	K_{IC} (MPa m$^{1/2}$)	p_{11}	p_{12}	q_{IC} (m$^{1/2}$)	$c_\parallel$	$c_\perp$	β
Plate Glass	73.9	0.23	1.52	0.75	0.06	0.16	3.8×10^{-6}	0.18	0.12	−0.42
PMMA	3.24	0.35	1.49	1.20	0.36	0.37	8.4×10^{-5}	0.41	0.40	−0.01
Araldite B	3.66	0.39	1.59	0.60	0.31	0.39	2.8×10^{-5}	0.49	0.44	−0.24

$$n_{\perp} = n_0(1-\sqrt{2c_{\perp}q_1}r^{-1/2}\{\cos(\theta/2)-\beta\sin\theta\cos[2(\omega-\varphi)]\}). \tag{11}$$

Further, we should note that for the case when $p_{11} = p_{12}$, $\beta = 0$, $c_{\perp} = c_{\parallel}$ and $n_1 = n_2 = n_3$. Hence, the index ellipsoid remains spherical and $n_{\parallel} = n_{\perp}$. In this case, the light is not split into two linearly polarized wavefronts. The incident wavefront maintains its initial polarization state while it traverses the near crack tip region. It does, however, deflect the same amount as the putative parallel wavefront.

Previous attempts (Fowlkes, 1975; Liang and Liechti, 1995) to calculate the deflection of light at a crack tip did not identify the existence of two possible wavefronts; as such, only one index of refraction was considered. An ad hoc relationship $n = n_0[1-\Delta]$ (where $\Delta = \varepsilon_{kk}$ = dilation) was used in those studies to model the index of refraction of the material. It is interesting to note that for a plane strain crack tip, since $\Delta = \varepsilon_{11}+\varepsilon_{22}$, the second equation of (10) can be rewritten exactly as $n_{\parallel} = n_0[1-c_{\parallel}\Delta]$, although $c_{\parallel} \neq 1$.

5. REVIEW OF GEOMETRICAL OPTICS OF ELECTROMAGNETIC WAVES IN ANISOTROPIC MEDIA

The equations of geometrical optics or "ray tracing" can be derived directly from Maxwell's equations by assuming that the wavelength of incident light is small compared to any characteristic dimension of the problem. The results of such an analysis are stated in this section. Readers interested in the detailed derivation can consult Kravtsov and Orlov (1990).

We begin with Maxwell's equations and the constitutive relations (1) and assume the vector quantities **B**, **H**, **D** and **E** vary sinusoidally with time. The wavefront is not constrained to be planar. Next, by expanding the vector quantities in a series in terms of powers of wavelength, it can be shown that, to first order, the wavefront propagates as if it were locally a plane wave. Hence, the result $|\mathbf{p}| = n$ from Section 2 holds for each of the two wavefronts. This result, known as the *eikonal equation* is valid for wave propagation in anisotropic, inhomogeneous media and can be written as

$$(p_1)^2+(p_2)^2+(p_3)^2 = n^2(\mathbf{x},\mathbf{p}) \tag{12}$$

where p_1, p_2 and p_3 are the components of the slowness vector in Cartesian coordinates.

Courant and Hibert (1966) discuss the general solution of the family of 1st order partial differential equations of which the eikonal equation is a member. When the general theory is applied to (12), the eikonal equation can be rewritten in terms of the following *characteristic system* of first order ordinary differential equations (Kravtsov and Orlov, 1990)

$$\frac{\mathrm{d}x_i}{\mathrm{d}s} = \cos\alpha\left[\frac{p_i}{n}-\frac{\partial n}{\partial p_i}\right]$$

$$\frac{\mathrm{d}p_i}{\mathrm{d}s} = \cos\alpha\frac{\partial n}{\partial x_i} \tag{13}$$

where

$$\cos\alpha = \left[1+\frac{\partial n}{\partial p_i}\frac{\partial n}{\partial p_i}\right]^{-1/2}. \tag{14}$$

The physical interpretation of the variables in the characteristic equations is as follows:

x corresponds, parametrically, to the path of the light ray

p = slowness vector, in direction of wave normal

s = path length along the light ray

α = angle between wavefront and light ray.

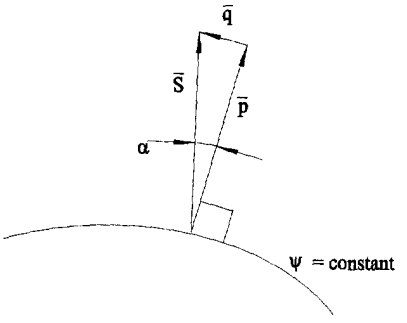

Fig. 5. Vector quantities relative to wavefront in a anisotropic medium.

Since n is a homogeneous function of degree zero in $\mathbf{p}$

$$p_i \frac{\partial n}{\partial p_i} = 0 \tag{15}$$

which implies that the vectors p_i and $\partial n/\partial p_i$ are orthogonal. As illustrated in Fig. 5, we define the vector

$$q_i = -n\,\partial n/\partial p_i. \tag{16}$$

The obvious physical interpretation of $\mathbf{q}$ is that $\mathbf{p}+\mathbf{q} = \mathbf{S}$, since α is the angle between the slowness vector, $\mathbf{p}$, and the ray direction given by the Poynting vector, $\mathbf{S}$.

In the next section, we will calculate the components of $\partial n/\partial p_i$ for the special case of a wavefront of light for which $\mathbf{p}$ is constrained to lie within a plane.

Since the eikonal equation (12) relates the slowness vector, $\mathbf{p}$, to the index of refraction it is evident that the *path of the wavefront* is determined by the index of refraction. The characteristic equations go one step further. They combine the effects of both the optical anisotropy and the change of index of refraction to calculate the *path of the light ray*.

6. LIGHT PROPAGATION IN NEAR CRACK TIP REGION OF A MODE I CRACK

With this background, the mathematical problem of calculating the *paths of the light rays* in the near crack tip region can be formulated. Since the index of refraction for the parallel wavefront is a special case of the index of refraction for the perpendicular wavefront (i.e. by setting $\beta = 0$), it suffices to calculate the path of the light ray of the perpendicular wavefront. Figure 6 shows the geometry being considered. Initially, the unit normal vector, $\mathbf{m}$, is directed in the positive x_2-direction. We introduce a new variable, ξ, which corresponds to the deflection of light from the nominal straight line path. A positive value of ξ indicates that the light deflects in the negative x_1-direction.

The initial position, x_1^0, is arbitrary. However in this analysis we will dwell on the

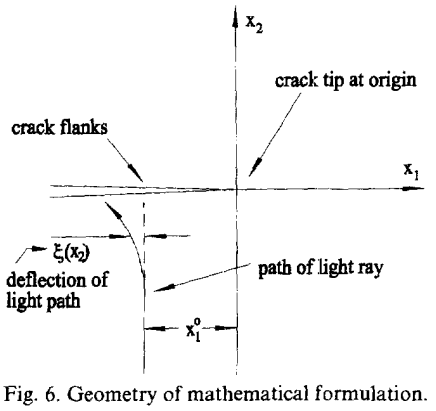

Fig. 6. Geometry of mathematical formulation.

special case of $x_1^0 = 0$, for which an analytical solution can be obtained. Numerical solutions for other initial positions are discussed later. The assumptions used to derive the analytical solution are:

1. incident wavefront of light nominally follows path $\theta = -\pi/2$
2. derivatives of index of refraction are always calculated on line $\theta = -\pi/2$
3. direction of wavefront normal is always $\omega = \pi/2$
4. small anisotropy (i.e. $c_\perp q_1 r^{-1/2} \ll 1$).

Implicit in Assumption 2 is that the analytical solution is valid only for $\xi(r) \ll r$. Also, since we have assumed a state of plane strain, the wavefront of incident light is constrained to propagate in the x_1–x_2 plane with $m_3 = 0$.

Referring to Fig. 3, the components of the vector $\partial n_\perp/\partial p_i$ are calculated by using that fact that $n_\perp$ is a homogeneous function of degree zero in $\mathbf{p}$, so that we can write

$$\frac{\partial n_\perp}{\partial p_i} = \frac{\partial n_\perp}{\partial \omega}\frac{\partial \omega}{\partial p_i} \tag{17}$$

where

$$\omega = \tan^{-1}\left(\frac{p_2}{p_1}\right). \tag{18}$$

The in-plane components of the vector $\partial n_\perp/\partial p_i$ then become

$$\begin{aligned}\frac{\partial n_\perp}{\partial p_1} &= \frac{-m_2}{n_\perp}\frac{\partial n_\perp}{\partial \omega}\\ \frac{\partial n_\perp}{\partial p_2} &= \frac{m_1}{n_\perp}\frac{\partial n_\perp}{\partial \omega}.\end{aligned} \tag{19}$$

Using Assumption 4, the binomial theorem and the Taylor expansion for cosine, (14) can be rewritten for the case of "small anisotropy" as

$$\alpha \approx \left|\frac{\partial n_\perp}{\partial \mathbf{p}}\right| = \frac{1}{n_\perp}\frac{\partial n_\perp}{\partial \omega}. \tag{20}$$

The characteristic system of differential eqns (13) can then be combined and rearranged to obtain

$$\begin{aligned}\frac{\mathrm{d}^2 x_1}{\mathrm{d}s^2} + \left(\frac{1}{n_\perp}\frac{\partial n_\perp}{\partial s}\right)\frac{\mathrm{d}x_1}{\mathrm{d}s} &= \frac{1}{n_\perp}\frac{\partial n_\perp}{\partial x_1} + \alpha\frac{1}{n_\perp}\frac{\partial n_\perp}{\partial x_2} + \frac{p_2}{n_\perp}\frac{\mathrm{d}\alpha}{\mathrm{d}s}\\ \frac{\mathrm{d}^2 x_2}{\mathrm{d}s^2} + \left(\frac{1}{n_\perp}\frac{\partial n_\perp}{\partial s}\right)\frac{\mathrm{d}x_2}{\mathrm{d}s} &= \frac{1}{n_\perp}\frac{\partial n_\perp}{\partial x_2} - \alpha\frac{1}{n_\perp}\frac{\partial n_\perp}{\partial x_1} - \frac{p_1}{n_\perp}\frac{\mathrm{d}\alpha}{\mathrm{d}s}.\end{aligned} \tag{21}$$

We now formulate the equations governing the behavior of light subject to the assumptions discussed above by combining (11) with (20) and (21). The quantities specific to this problem on the line $\theta = -\pi/2$ with nominal direction of wavefront propagation $\omega = \pi/2$ are

$$\begin{aligned}n_\perp &= n_0\,[1 - c_\perp q_1(1-\beta)r^{-1/2}]\\ \frac{\partial n_\perp}{\partial x_1} &= -\frac{1}{2}n_0 c_\perp q_1(1-3\beta)r^{-3/2}\\ \left\langle\frac{\partial n_\perp}{\partial x_2} = -\frac{1}{2}n_0 c_\perp q_1(1-\beta)r^{-3/2}\right\rangle\\ \langle\alpha = -2c_\perp q_1\beta r^{-1/2}\rangle.\end{aligned} \tag{22}$$

The resulting equations are linearized by replacing $n_\perp$ with n_0 whenever $n_\perp$ occurs in a denominator and by assuming that $p_2 \approx n_\perp$ for $\alpha \ll 1$. Finally substituting $\xi = -x_1$ and $r = -s$ into the first equation of (21) yields the governing equation for the deflection of the light as it approaches a crack tip

$$\frac{d^2\xi}{dr^2} + \left[\frac{1}{2}c_\perp q_I(1-\beta)\right] r^{-3/2}\frac{d\xi}{dr} = \frac{1}{2}c_\perp q_I(1-\beta)r^{-3/2} - (c_\perp q_I)^2\beta(1-\beta)r^{-2} \tag{23}$$

with initial conditions

$$\langle \xi(r = r_0) = 0 \rangle$$
$$\left\langle \left.\frac{d\xi}{dr}\right|_{r=r_0} = -2c_\perp q_I \beta r_0^{-1/2} \right\rangle. \tag{24}$$

The initial radius, r_0, is the largest radius at which the singular term in the strain field dominates (i.e. the radius of the K-field). As such, r_0, is a function of the geometry of a specimen. The initial condition for the slope is determined by the angle α at $r = r_0$.

The equation governing the light path in the x_2-direction can be obtained in a similar manner. It is satisfied to the order $O(c_\perp^2 q_I^2 r_0^{-1})$, so (23) and (24) suffice to calculate the light path.

If the equations are made non-dimensional by scaling r with r_0 and ξ with q_I^2, it can be shown that the second terms of both sides (23) are negligible when compared with the first terms of both sides of the equation. Then (23) reduces to

$$\frac{d^2\xi}{dr^2} = \frac{1}{2}c_\perp q_I(1-\beta)r^{-3/2}. \tag{25}$$

The rate of deflection and the total deflection of the light ray for the perpendicular wavefront subject to initial conditions (24) can then be found by simple integration. The results (expressed in dimensional variables) at any radius $0 < r < r_0$ are

$$\frac{d\xi}{dr} = -2c_\perp q_I \beta r^{-1/2} - (1-3\beta)c_\perp q_I r_0^{-1/2}\left[\left(\frac{r}{r_0}\right)^{-1/2} - 1\right] \tag{26}$$

$$\frac{\xi(r)}{c_\perp q_I r_0^{1/2}} = -4\beta\left[\left(\frac{r}{r_0}\right)^{1/2} - 1\right] + (1-3\beta)\left[\left(\frac{r}{r_0}\right)^{1/2} - 1\right]^2. \tag{27}$$

In considering the physical origin of the terms in the solutions (26) and (27), we must keep in mind that two processes are at work to affect the path of the light ray. The first is the strain induced optical anisotropy, characterized by β, which causes the light ray to propagate in a direction that is not normal to the wavefront. The second is the inhomogeneity of the index of refraction, characterized by $c_\perp q_I r^{-1/2}$, which causes the wavefront itself to change direction.

We note that the first term on the right hand side of (26) is identical to the expression for α in (22). It is evident that this term arises solely from the effects of anisotropy and represents the rate of light deflection that would occur if the wavefront were to remain plane throughout the course of its journey toward the crack tip (i.e. if the index of refraction were homogeneous). However, it is impossible to completely separate the effects of anisotropy and inhomogeneity because, as the expression for α in (22) shows, the degree of anisotropy is a function of position. That is, the anisotropy itself is inhomogeneous.

The second term on the right hand side of (26) arises from the effects of the inhomogeneous index of refraction which causes an initially plane wave to become non-planar.

Thus, the direction of wavefront propagation changes. The numerical factor of $(1-3\beta)$ is due to the coupling between the inhomogeneity and the anisotropy.

The effect of the inhomogeneity can be seen most clearly in the case of the parallel wavefront where the index of refraction is isotropic. The rate of deflection and the total deflection of the light ray of the parallel wavefront are found by setting $\beta = 0$ and substituting $c_\parallel$ for $c_\perp$ in (26) and (27).

We now have the solution for the path of the light ray of both the parallel and perpendicular wavefronts. It is evident that the two light rays deflect different amounts. The total deflection of each ray when it reaches the crack flanks is given as

$$\xi_\parallel^{\text{total}} = \xi_\parallel(r=0) = c_\parallel q_1 r_0^{1/2}$$
$$\xi_\perp^{\text{total}} = \xi_\perp(r=0) = c_\perp q_1(1+\beta) r_0^{1/2}. \tag{28}$$

At this point we should recall that solutions (26) through (28) were obtained by neglecting two terms in the governing eqn (23). We must ask ourselves whether the neglected terms are important, considering the fact that, even though the expression for deflection in (27) remains bounded, the expression for the slope of deflection in (26) is singular. Hence, in Appendix A, we calculate the exact solution for the deflection and the slope of deflection of the light taking into account all the terms of (23).

The exact expression shows that as $r \to 0$ the deflection of the light ray diverges as $\xi \propto \exp[c_\perp q_1(1-\beta) r^{-1/2}]$. This would seem to indicate that the approximate solution (27) is not valid. However, an asymptotic approximation of the singularity in the exact solution for ξ as $r \to 0$ shows that ξ remains finite for all $r > (c_\perp q_1(1-\beta))^2$. Using Table 1, we see that the deflection for a typical material will remain finite for any $r > 10^{-10}$ m. Since this dimension is several orders of magnitude smaller than the wavelength of the incident light, we conclude that (27) is valid on physical grounds.

Similarly from the exact analysis, we note that the approximate solution for the slope of deflection in (26) is valid as $r \to 0$ as long as $r > (c_\perp q_1(1-\beta))^2$. Using Table 1, the slope of the light rays in a typical material at a radius equal to the wavelength of the incident light is of the order $O(10^{-2})$. This small angular deflection justifies Assumption 3. Finally, Appendix A also shows that Assumption 2 is valid for $r > 0.01 r_0$ and that light deflection which occurs at smaller radii does not significantly affect the solution.

The analytical results are valid only for initial conditions $x_1^0 = 0$. In order to calculate the path of light rays with other initial conditions, we numerically solved (21) subject to (24) using the fourth order Runge–Kutta method with variable step size. Plots of the analytical and numerical results are shown in Fig. 7, for the parallel wavefront, and Fig. 8, for the perpendicular wavefront for the choice $\beta = 0.25$. The figures can be interpreted as being the actual path the light rays follow as they approach the crack which has its tip at $x_1 = 0$ and its flanks coinciding with the negative x_1-axis. Each line corresponds to a light ray approaching the crack from the positive x_2-direction. The leftmost line on each figure is the ray that corresponds to the analytical solution.

As is evident in Fig. 7 and Fig. 8, the light rays associated with the perpendicular wavefront have a non-zero initial slope which is consistent with wave propagation in anisotropic media. The light rays associated with the parallel wavefront have an initial slope of zero which is consistent with wave propagation in isotropic media.

Figure 9 plots the total deflection for light rays which approach the crack with normal incidence but from initial positions either in front of or behind the crack tip.

7. IMPLICATIONS FOR CRACK OPENING INTERFEROMETRY

The light associated with each wavefront reflects from both crack flanks and interferes to form a set of fringes. Since the wavefronts are polarized in mutually orthogonal directions, each wavefront will interfere only with itself; thus two sets of interference fringes are generated.

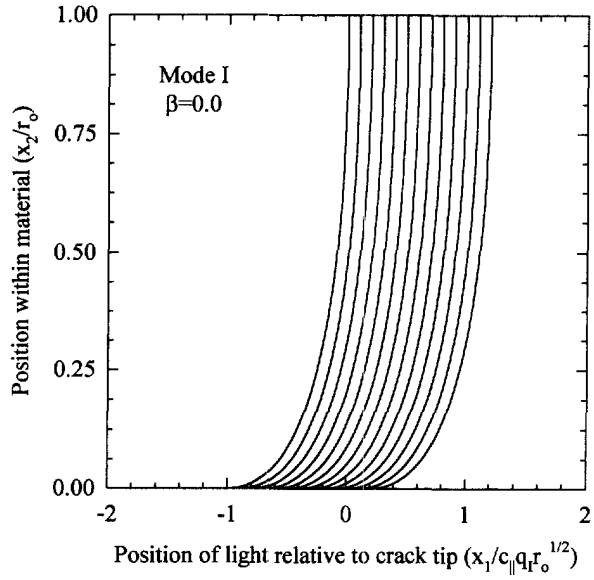

Fig. 7. Path of light ray polarized in plane parallel to crack front.

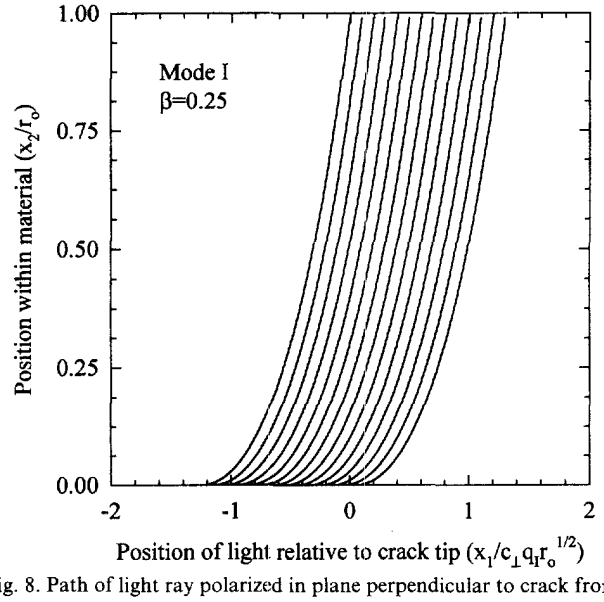

Fig. 8. Path of light ray polarized in plane perpendicular to crack front.

The intensity of an interference fringe at a point depends upon the local normal crack opening displacement. Assuming that both wavefronts initially have the same intensity, the intensity of each sets of fringes will be the same at each point. Therefore, the two sets of fringes coincide and appear identical to an observer situated inside the crack that is incapable of distinguishing polarization (i.e. photographic film, CCD arrays, retinas, etc). The resulting "single" set of interference fringes is localized in the region of the crack flank closest to the incident light source and is shown symbolically in Figure 1 as a set of small circles.

In crack tip interferometry, the observer is usually in the same location as the light source and must look at the fringes through the transparent material. An image of the fringes is transmitted to the observer along the same path as the incident light. Therefore, two images of the single set of interference fringes are transmitted back to the observer. The observer can distinguish between the two images by looking through a properly oriented polarizer.

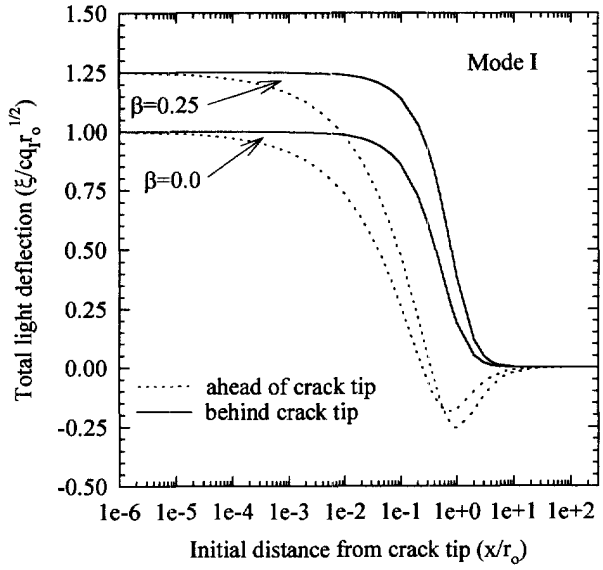

Fig. 9. Total deflection of light rays with other initial conditions.

An observer would record two sets if the difference between $\zeta_{\parallel}^{\text{total}}$ and $\zeta_{\perp}^{\text{total}}$ in (28) is sufficiently large. This could lead to erroneous measurements of normal crack opening displacement if the observer is not aware that two sets of fringes exist.

Also, this phenomenon could be exploited to directly obtain the value of the stress intensity factor, K_{I}, from (28) by simply measuring $\zeta_{\parallel}^{\text{total}} - \zeta_{\perp}^{\text{total}}$. In addition, if the light deflection due to a Mode II loading were known, one could obtain the values of both K_{I} and K_{II} from crack opening interferometry. In that case, it would be necessary to measure K_{I} from the normal crack opening displacement and to infer K_{II} from an expression analogous to (28) which would account for both Mode I and Mode II loading.

If one were to attempt such measurements, it would be necessary to estimate the value of r_0, probably with the finite element method. We can evaluate the feasibility of this technique by calculating the difference in deflection between the two rays for the materials listed in Table 1. If we arbitrarily assume that the radius of the K-field is $r_0 = 0.01$ m, Table 2 shows the total light deflections as well as the relative deflections.

Under the assumptions made, the absolute light deflection for some materials (e.g. PMMA) is large enough to be measured. However, the difference in the light deflection is too small to be measured for all the materials considered. In fact, the difference in light deflection would have to be at least a factor of 15 times larger to be experimentally significant. It seems unlikely that this method could be used to make meaningful measurements.

Finally, in those materials for which the absolute light deflection is large enough to be measured, the crack tip will change its apparent position relative to the observer. Similarly, the interference fringes will change their apparent positions by an amount that is a function of distance from the crack tip. This could result in an apparent distortion (i.e. stretching or compressing) of the interference fringes which would lead to errors in extracting the stress intensity factor. Figure 9 shows that the fringes within the range $r < 10^{-2} r_0$ all shift approximately the same amount, so that this effect need not be considered.

Table 2. Deflection of light for commonly used materials

Material	$\zeta_{\parallel}^{\text{total}}$ (m)	$\zeta_{\perp}^{\text{total}}$ (m)	$\zeta_{\parallel}^{\text{total}} - \zeta_{\perp}^{\text{total}}$ (m)
Plate Glass	7×10^{-8}	3×10^{-8}	4×10^{-8}
PMMA	3.4×10^{-6}	3.3×10^{-6}	1×10^{-7}
Araldite B	1.4×10^{-6}	9×10^{-7}	5×10^{-7}

8. RESULTS AND CONCLUSIONS

The behavior of light at a plane strain crack tip is surprisingly complex. An incident light wavefront is split into two linearly polarized light wavefronts: one polarized in a plane parallel to the crack front; the other polarized in a plane perpendicular to the crack front. Each wavefront experiences a different index of refraction, and hence, the associated light rays deflect different amounts.

The exact relationship between index of refraction and position for a Mode I crack tip is derived for both wavefronts. The problem reduces to one of electromagnetic wave propagation in an anisotropic, inhomogeneous medium.

The groups of mechanical and optical properties relevant to light deflection in crack tip interferometry are identified and tabulated for commonly used materials.

The light path for both light rays is calculated analytically for the special case of a light wavefront that would, in an unloaded state, approach the crack in the direction perpendicular to the crack flanks and strike the crack tip. Hence, an expression for the total light deflection of both light paths at the crack tip is obtained in terms of the previously identified material parameters. In addition, the system of equations is solved numerically to investigate the behavior of light wavefronts with other initial positions.

The results show that for some materials and specimen geometries, the absolute deflection of each light ray is large enough to be measured. But the relative deflection (i.e. the difference in deflection between the two light rays) is too small to be measured. The main effect that this phenomenon has on crack opening interferometry is to cause a shift in the apparent position of the crack tip. It is shown that this shift will not affect the interpretation of the interference fringes in terms of crack opening displacement.

These results are also of interest because they are an analytical solution to Maxwell's equations in an anisotropic, inhomogeneous medium.

This analysis did not account for variations in the indices of refraction due to temperature changes. This may be important if the fracture process occurs dynamically or if large plastic zones are formed.

Acknowledgements—This work was supported through an AASERT grant by the Office of Naval Research, Mechanics Division, grant N00014-93-1-1037 and by ONR grant N00014-90-J-1379. The author wishes to thank Prof. J. R. Rice for advice, guidance and support.

REFERENCES

Born, M. and Wolf, E. (1993) *Principles of Optics*, sixth (revised) edn. Pergamon Press, Oxford.

Courant, R. and Hilbert, D. (1996) *Methods of Mathematical Physics, vol II, Partial Differential Equations*. Interscience Publishers, New York.

Fowlkes, C. W. (1975) Crack opening interferometry—the effects of optical refraction. *Engineering Fracture Mechanics* **7**, 689–691.

Günter, P. and Zgonik, M. (1991) Clamped-unclamped electro-optic coefficient dilemma in photorefractive phenomena. *Optics Letters* **16**, 1826–1828.

Kalthoff, J. F. (1993) Shadow optical method of caustics. In *Handbook on Experimental Mechanics*, ed. A. S. Kobayashi, ch. 9. VCH Publishers, New York.

Kanninen, M. F. and Popelar, C. H. (1985) *Advanced Fracture Mechanics*. Oxford University Press, UK.

Kravtsov, Yu. A. and Orlov, Yu, I. (1990) *Geometrical Optics of Inhomogeneous Media*. Springer-Verlag, Berlin.

Lawn, B. (1993) *Fracture of Brittle Solids*, second edn. Cambridge University Press, UK.

Liechti, K. M. (1993) On the use of classical interferometry techniques in fracture mechanics. In *Experimental Techniques in Fracture*, ed. J. S. Epstein, ch. 4. VCH Publishers, New York.

Liang, Y.-M and Liechti, K. M. (1995) Toughening mechanisms in mixed-mode interfacial fracture. *International Journal of Solids and Structures* **32**, 957–978.

Nye, J. F. (1972) *Physical Properties of Crystals*. Oxford University Press, UK.

Watson, M., Cebon, D., Ashby, M. F. *et al.* (1994) *Cambridge materials selector, version* 2.0, Granta Design, Ltd., Cambridge, UK.

APPENDIX A: EXACT EXPRESSIONS FOR DEFLECTION OF LIGHT RAY

There is no ξ term in (23), so the equation immediately reduces to a first order ordinary differential equation by defining the *slope* as

$$s = \frac{d\xi}{dr}. \tag{A.1}$$

The resulting equation can be directly integrated by identifying the integrating factor

$$\mu(r) = \exp[-c_\perp q_1(1-\beta)r^{-1/2}]. \tag{A.2}$$

Thereupon, (23) can be written as

$$\frac{d}{dr}[s\mu(r)] = \mu(r)\left[\frac{1}{2}c_\perp q_1(1-\beta)r^{-3/2} - (c_\perp q_1)^2\beta(1-\beta)r^{-2}\right]. \tag{A.3}$$

The exact solutions of the rate of deflection and the total deflection at any radius $0 < r < r_0$ subject to initial conditions (24) are

$$\left(\frac{1}{c_\perp q_1 r_0^{-1/2}}\right)\frac{d\xi}{dr} = -2\beta\left(\frac{r}{r_0}\right)^{-1/2} + \frac{(1-3\beta)}{\gamma}\left\{1-\exp\gamma\left[\left(\frac{r}{r_0}\right)^{-1/2}-1\right]\right\} \tag{A.4}$$

and

$$\frac{\xi(r)}{c_\perp q_1 r_0^{1/2}} = -4\beta\left[\left(\frac{r}{r_0}\right)^{1/2}-1\right]+\left(\frac{1-3\beta}{\gamma}\right)\left(\frac{r}{r_0}\right)\left\{1-\exp\gamma\left[\left(\frac{r}{r_0}\right)^{-1/2}-1\right]\right\}$$
$$+(1-3\beta)\left\{1-\left(\frac{r}{r_0}\right)^{1/2}\exp\gamma\left[\left(\frac{r}{r_0}\right)^{-1/2}-1\right]\right\}+(1-3\beta)\gamma\exp(-\gamma)I \tag{A.5}$$

where

$$I = -\frac{1}{2}\ln\left(\frac{r}{r_0}\right)+\frac{\gamma}{1\cdot 1!}\left[\left(\frac{r}{r_0}\right)^{-1/2}-1\right]+\cdots+\frac{\gamma^n}{n\cdot n!}\left[\left(\frac{r}{r_0}\right)^{n/2}-1\right]+\cdots$$

and

$$\gamma = c_\perp q_1 r_0^{-1/2}(1-\beta).$$

The deflection formally diverges exponentially with decreasing radius (i.e. with singularity $\xi \propto \exp[c_\perp q_1(1-\beta)r^{-1/2}]$). In order to investigate the behavior of the singularity in (A.5), we integrate (A.4) by parts to obtain an asymptotic approximation for ξ as $r \to 0$. It is the form

$$\xi(r) \sim \frac{e^{\gamma x}}{x^3} = x^{-3}+\gamma x^{-2}+\cdots+\frac{\gamma^n x^{n-3}}{n!}+\cdots \tag{A.6}$$

where

$$x = \left(\frac{r}{r_0}\right)^{-1/2}.$$

A conservative criterion which ensures a finite deflection is $\gamma x < 1$. This corresponds to

$$\frac{r}{r_0} > [c_\perp q_1 r_0^{-1/2}(1-\beta)]^2. \tag{A.7}$$

Using representative material properties from Table 1, it is evident that the exact expressions predict that the deflection and slope diverge on a scale that is less than that of an atomic spacing. Indeed, when the exact solution (A.4) is evaluated numerically for $\gamma = O(10^{-5})$, the deflection diverges at $r/r_0 = O(10^{-12})$. Since the wavelength of light is several orders of magnitude greater than this length, the singular solution does not apply. Therefore, the approximate expressions for the rate of deflection (26) and for the path of the light ray in (27) are physically valid.

We also estimate the slope of the light ray as it approaches the crack tip. It can be shown from (A.4) that if (A.7) holds, the slope is $d\xi/dr \propto -c_\perp q_1(1-\beta)r^{-1/2}$. As an example, the slope of the light ray for PMMA at a radius equal to the wavelength of the incident light is of the order $O(10^{-2})$.

As a result of Assumption 2 in Section 6, the solution is only valid for $\xi(r) \ll r$. If the cut-off value for validity is chosen, arbitrarily, as $\xi(r)/r = 10^{-2}$, typical values from Table 1 indicate that the domain of validity is $r > 0.01r_0$. At smaller radii, the expressions analogous to those in (22) would be augmented with trigonometric functions in θ that are of order unity. Therefore, the overall order of magnitude of the terms would still be determined by the radius. Hence, the final deflection will be of the same order of magnitude calculated in the above solutions. This finding is reinforced by the numerical calculations presented in Fig. 9.